

Comparative anatomical and histological study of plastinated and non-plastinated organs of one-humped camel (*Camelus dromedarius*)

Esraa Y. Medina^{1*}, Hatem Bahgat¹, Ahmed A. Kassab¹, Anwar A. El-Shafey^{1,2}

¹Department of Anatomy and Embryology, Faculty of Veterinary Medicine, Benha University, Toukh 13736, Egypt.

²Department of Basic Veterinary Sciences, Faculty of Veterinary Medicine, Delta University for Science and Technology, Dakahlia, Egypt.

ARTICLE INFO

Received: 01 April 2025

Accepted: 05 May 2025

*Correspondence:

Corresponding author: Esraa Y. Medina
E-mail address: esraa.yasser@fvmt.bu.edu.eg

Keywords:

Dromedary camel, Plastination, Transmission Electron Microscopy, Spleen, Testis

ABSTRACT

Formalin, commonly used as an embalming fluid for tissue preservation, poses significant risks to the public health of humans and animals. The present study aimed to focus on the Elnady plastination method for tissue preservation and examined the macro and microscopic changes in two organs before and after the plastination. Spleen and testis samples from six one-humped camels were used in this study. Plastination process included formalin fixation, acetone dehydration, glycerin impregnation, and cornstarch curing. The gross morphological changes and weights of the spleen and testis were measured after each treatment phase. The spleen turned dark brown after the glycerin phase, while the testicular capsule became more transparent. Shrinkage was noted as 23.16% in the spleen and 31.57% in the testis. Both light and transmission electron microscopical (TEM) results confirmed the shrinkage, especially in the collagen fibers, that showed reduction in their amount and formation of spaces between the cells in both the spleen and testis.

Introduction

There is no doubt that tissue decomposition is an unavoidable process that occurs after death when the body breaks down due to the activity of bacteria, enzymes, and environmental factors. These processes are part of natural deterioration, and they cause tissue degradation (Dent *et al.*, 2004). Therefore, it became essential to discover a method to prevent cadavers from decaying, and the first and most well-known technique was the art of mummification practiced by the ancient Egyptians. They used certain organic substances derived from crops, which had antibacterial properties, to preserve the bodies. For example, the choice of Natron salt, which was crucial for drying the body, may have been driven by its exceptional ability to break down adipose tissue (Abdel-Maksoud and El-Amin, 2011). As science has advanced over time, morphologists have consistently attempted to find methods to preserve biological specimens while maintaining their original characteristics. As a result, they have turned to tissue preservation agents like formaldehyde, which remains one of the most commonly used embalming substances for preservation in educational settings (Baygeldi *et al.*, 2022).

However, the harmful effects of formalin have been proven, as cited by Elshaer and Mahmoud (2017), who found that over 50% of employees and medical students in anatomy departments for over 10 years are at risk of formaldehyde exposure. They suffered from respiratory irritation, eye problems, and long-term health issues like cancer and neurological disorders. As a result, anatomists explored the embalming methods that minimized health risks while preserving specimens to resemble living tissue longer (Balta *et al.*, 2015).

The plastination technique is a method employed to preserve biological tissues by substituting water and lipids with a long-lasting polymer such as silicon to produce dry, durable specimens for anatomical study (Yunus *et al.*, 2022). However, the plastination process demands specialized equipment such as a vacuum chamber, gas curing chamber, deep

freezer, and various tools like PVC pipes, and costly polymers. That leads to a significant initial investment for a plastination lab (Reina-De La Torre *et al.*, 2004). However, the Elnady technique employs readily available, low-cost requirements (Elnady, 2016).

Shrinkage is the one of changes that occur in samples traditionally plastinated using silicone, (Sora and Traxler, 1999). While, histological alterations including artifacts, loss of nuclear clarity and sharpness reduction of the architectures, were observed in liver, lung, and kidney of the goat (Islam, 2021). On the other hand, neither macroscopic nor histological changes that occurred in the plastinated specimens using the Elnady technique have been adequately investigated in previous studies according to the available literature.

The objective of our study was to monitor the macroscopic changes especially the shrinkage of plastinated specimens using statistical analysis to calculate the shrinkage percentage at each stage of the Elnady technique, applied to the spleen and testis of the one-humped camel. Furthermore, utilizing light microscopy and transmission electron microscopy (TEM) to conduct a histological comparison between plastinated and non-plastinated tissues.

Materials and methods

Ethical Approval

All experimental procedures were conducted following international guidelines for laboratory animal care and received approval from the Research Ethical Committee of the Faculty of Veterinary Medicine, Benha University (Ethical Approval Number: BUFVTM 24-09-23).

Samples preparation

The spleens and testes of six (five-year-old), apparently healthy cam-

els were collected after slaughtering at Toukh abattoir in Qalyubia, Egypt. Tissue samples (1×1 cm) were taken before plastination and maintained in 5% formalin for histological investigation, while smaller slices (0.5×0.5 cm) were prepared for transmission electron microscopy (TEM) inspection after being washed and fixed in glutaraldehyde. The organs were then transferred for plastination treatments using the Elnady technique as cited by Elnady (2016). From the plastinated organs, similar specimens have been taken for histological and TEM evaluation.

Plastination technique steps

Formalin fixation

Firstly, the spleens and testes were directly injected with formalin to infiltrate the tissues (Ostrom, 1987). Then, they were immersed in 5% formalin solution for two weeks.

Acetone dehydration

The specimens were removed from the formaldehyde container, rinsed with water, and allowed to drain. It was then placed in a sealed container with a 99.9% acetone bath for dehydration at room temperature. A weight was added to prevent floating. The acetone percentage was monitored and adjusted using an acetometer until it stabilized. The organs were then transferred to a second acetone bath. The completion of the dehydration process was for two weeks and was confirmed by the change in acetone color from colorless to straw yellow, indicating successful dehydration (Elnady, 2016; El-Shafey *et al.*, 2022).

Glycerin impregnation

The specimens were drained for an hour and then placed on a metal framework to speed up acetone evaporation. Next, the organs were immersed in a 99.9% glycerin bath for 15 days to replace the acetone. A decrease in glycerin viscosity indicates successful tissue impregnation (Bernal *et al.*, 2022).

Cornstarch curing

Each organ was pressed with tissue paper after removal from the glycerin solution and left to dry. To avoid starch buildup from glycerin leakage, the organs were wrapped in cotton sacks filled with cornstarch powder. A gentle massage was suggested. The hardening time varied with size, requiring multiple powder changes while moisturizing with glycerin.

Organs' storage

Once cured, excess starch powder was brushed off. The specimens were then stored in a sealed plastic box in a clean, dry area. They could be handled directly as their surfaces were dry.

Gross anatomical examination and statistical analysis

Organs' gross morphology and weights before and after each plastination step were recorded and compared with fresh ones for statistical monitoring. Data were analyzed using one-way ANOVA in SPSS (Version 25), with LSD and Duncan tests to assess mean differences set at $p \leq 0.05$ for significance.

Light microscope examination

To prepare the tissues for observation under a light microscope, the non-plastinated specimens were first fixed in 5% formalin for 72 hours.

Then, they are dehydrated by passing through ascending grades of alcohol, then cleared with xylene. The tissues were subsequently infiltrated with different grades of melted paraffin. Finally, 5-6 μm thick sections were sliced from both plastinated and non-plastinated tissues using a microtome, then processed and stained with hematoxylin and eosin (H&E) and Masson's trichrome stain (MTC) (Bancroft and Gamble, 2008).

Transmission electron microscopy

Both plastinated and non-plastinated specimens follow the electron microscope protocol, starting with fixation in 2.5% buffered glutaraldehyde in 0.1 M PBS (pH 7.4) at 4°C for 2 hours. The specimens were washed three times with PBS for 10 minutes each. Next, they underwent post-fixation in 1% osmium tetroxide for 30 minutes, followed by three PBS washes. They were dehydrated through increasing concentrations of ethyl alcohol (30%, 50%, 70%, 90%, and absolute alcohol), each for 30 minutes. After dehydration, the specimens were infiltrated with acetone for 1 hour and embedded in Araldite 502 resin. The plastic molds were sectioned with a LEICA ultramicrotome and stained with uranyl acetate, followed by counterstaining with lead citrate (Tizro *et al.*, 2019). The specimens were then examined and photographed using a JEOL JEM-100 SX electron microscope at the Faculty of Medicine, Tanta University, Egypt.

Results

Morphology and statistical analysis results

The gross anatomical results of both plastinated camel spleens and testes were compared with fresh ones. The fresh non-plastinated camel's spleen had a C-shape and a reddish-brown color, while the camel testis was white and covered by a thick connective tissue capsule, the tunica albuginea. The plastinated specimens showed a change in organ coloration during each step of the plastination treatment. The color ranged from pale color after the formalin and acetone phases to transparent as in the testis and the appearance of dark brown patches as on the spleen after the glycerin impregnation phase (Fig. 1).

Table 1 shows the statistical monitoring of the mean weights of plastinated spleen and testis. A significant decrease in weight was observed at different stages of plastination except for the formalin fixation step in which the testis exhibited a noticeable increase in weight, unlike the spleen, which showed a reduction. The shrinkage percentages, comparing fresh organs to each plastination stage, were outlined in Table 2 and Figure 2. At the end of the plastination process, the spleen shrunk by approximately 23.16%, while the testis by 31.57%.

Table 1. Showing changes in the spleen and testis weights at various plastination process steps.

Different steps of plastination	Spleen weight (g)	Testis weight (g)
Fresh	475.83±38.00 ^a	155.83±24.98 ^a
Formalin	462.50±33.73 ^a	163.33±27.33 ^a
Acetone 1	422.50±25.25 ^b	152.50±23.61 ^{ab}
Acetone 2	402.50±17.25 ^{bc}	141.67±21.60 ^{ab}
Glycerin	387.50±12.55 ^{cd}	123.33±23.59 ^{bc}
Starch	364.17±11.14 ^d	107.50±25.64 ^c

Values are presented as means ± standard deviation. Means with different superscript letters in the same column are considered significantly different ($P \leq 0.05$).

Spleen

Light microscopic results

The non-plastinated camel spleen was surrounded by a thick capsule with distinct outer and inner layers. The outer layer mainly consisted of

connective tissue (collagen, elastic, and reticular fibers) and a few smooth muscle cells. The inner layer primarily consisted of smooth muscle cells supported by fibers. Subcapsular blood sinuses extended beneath the capsule. The splenic parenchyma included white and red pulp (Fig. 3A). Collagen fibers surrounded the central arteriole in the white pulp and were scattered throughout the red pulp, providing structural support (Fig. 3C). The white pulp contained lymphoid follicles around the central arteriole, while the red pulp had splenic cords filled with blood cells (red blood cells, macrophages, lymphocytes, plasma cells), blood sinusoids, and collagen fibers support cells (Fig. 3E& G). Conversely, the plastinated spleen showed shrinkage of the outer connective tissue layer of the capsule and widening of the subcapsular sinus (Fig. 3B). The splenic parenchyma showed a normal arrangement of white and red pulp cells with shrinkage of collagen fibers around the central arteriole (Fig. 3D). Additionally, displayed typical cellular structure within the splenic tissue (Fig. 3F). The high power of red pulp exhibited widening of sinusoidal spaces (Fig. 3H).

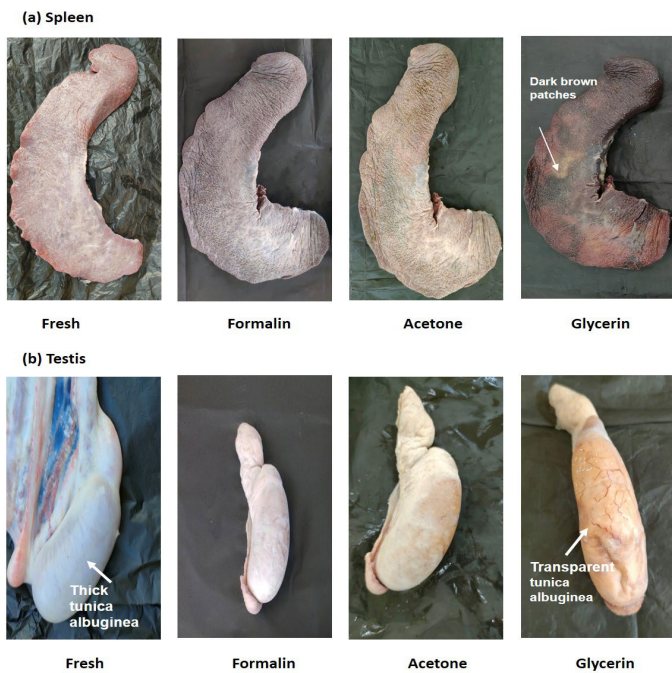


Fig. 1. The morphological color changes of the spleen and testis during different phases of plastination treatment.

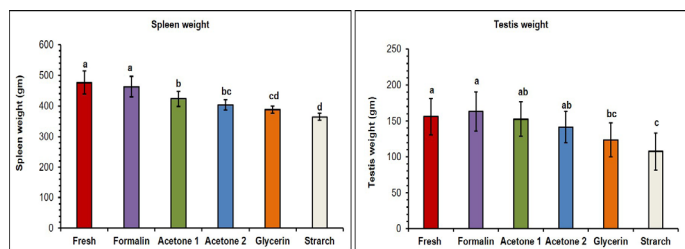


Fig. 2. Graphical illustration of statistical analysis of the spleen and testis weights at different phases of the plastination process.

Table 2. Percentage of spleen and testis shrinkage in each plastination step compared to a fresh specimen.

	Spleen		Testis	
	Percentage of shrinkage	95% Confidence Interval for Mean (Lower Bound- Upper Bound)	Percentage of shrinkage	95% Confidence Interval for Mean (Lower Bound- Upper Bound)
A (fresh- formalin)	2.75	1.57-3.94	-4.72	(-5.97)-(-3.46)
B (fresh- acetone1)	11.08	8.86-13.31	2.03	(-0.75)-4.80
C (fresh- acetone2)	15.18	11.40-18.97	8.89	4.30-13.48
D (fresh- glycerin)	18.28	13.76-22.81	21.06	15.68-26.44
E (fresh- starch)	23.16	18.00-28.31	31.57	23.95-39.19

Means of different percent of shrinkage in the same column are significantly different (P<0.05).

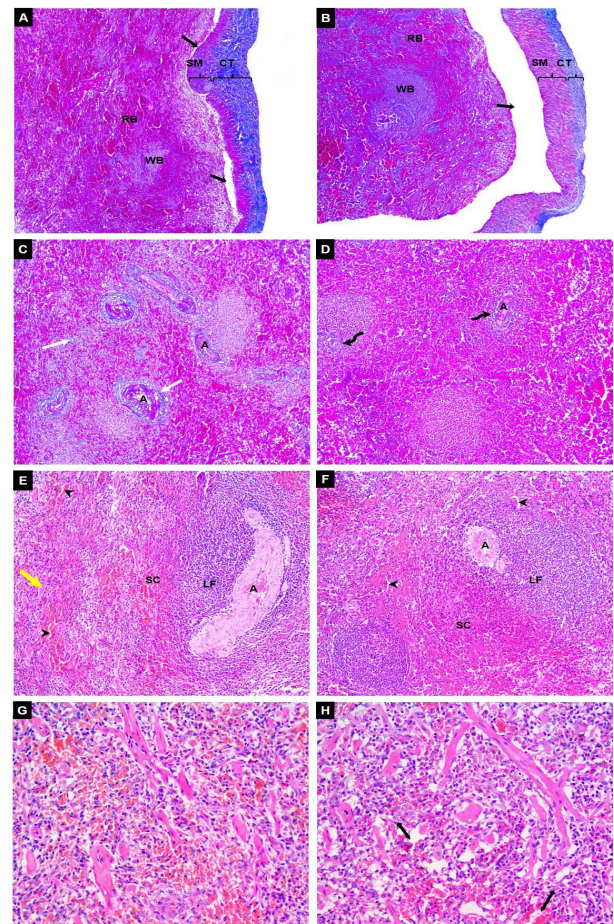


Fig. 3. Photomicrographs of plastinated and non-plastinated spleen. (A) Non-plastinated spleen showing splenic capsule with outer connective tissue (CT), inner smooth muscle cells (SM), and the subcapsular sinus (black arrow), white pulp (WP), and red pulp (RP). (B) Plastinated spleen with shrinkage of the outer connective tissue and widening of the subcapsular sinus. (C) Non-plastinated parenchyma showing collagen fibers (white arrow) and central arteriole (A). (D) Plastinated parenchyma showing thinning of collagen fibers (curved arrow). (E) Non-plastinated parenchyma with lymphoid follicles (LF), central arteriole (A), splenic cords (SC), blood sinusoids (arrowhead), and collagen fibers (yellow arrow). (F) Plastinated specimen showing typical cellular organization within splenic parenchyma. (G) High magnification of non-plastinated red pulp cells, sinusoids, and collagen fibers. (H) High magnification of plastinated red pulp showing widened blood sinusoids (diamond arrow). (A, B) X100 magnification, MTC staining; (C, D) X200 magnification, MTC staining; (E, F) X200 magnification, H&E staining; (G, H) X400 magnification, H&E staining.

Transmission electron microscopic results

TEM examination of the non-plastinated spleen camel revealed various cell structures, including lymphocyte which showed spherical nucleus containing chromatin. The cytoplasm was usually sparse and contained small amounts of visible organelles such as mitochondria, and ribosomes encircled by clear plasma membrane (Fig. 4A). The red blood cells, situated between the lymphocytes, were firmly attached to the extracellular matrix (Fig. 4C). The macrophage exhibited a typical structure of a kidney-shape nucleus with a typically well-developed rough endoplasmic reticulum (RER) that appeared as a network of flattened sacs studded by

the ribosome (Fig. 4E). Conversely, the plastinated spleen lymphocytes exhibited shrunken and reduction of the cytoplasmic amount leading to the formation of peri-nuclear space surrounding the nucleus (Fig. 4B). Additionally, the intercellular spaces between the red blood cells and lymphocytes became expanded (Fig. 4D). Also, the membranes of the RER of the macrophage became stretched out and appeared dilatations and widenings between the sacs of RER (Fig. 4F).

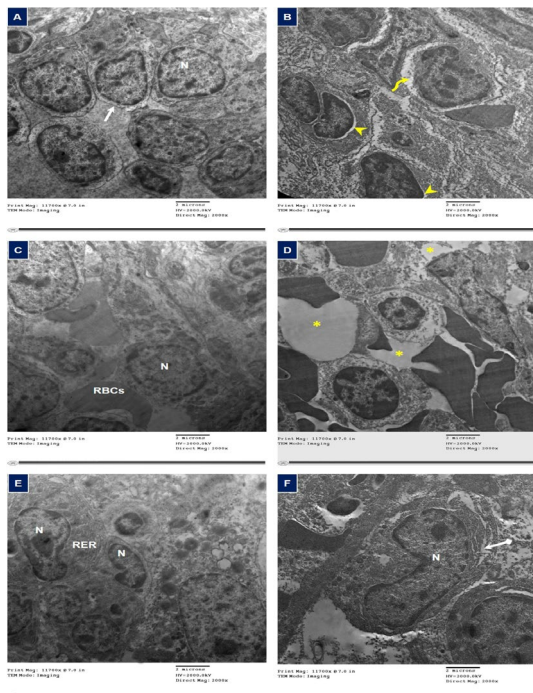


Fig. 4. Transmission electron micrographs of plastinated and non-plastinated spleen. (A) Non-plastinated lymphocytes with spherical nucleus (N), visible cytoplasmic membrane (arrow). (B) Plastinated lymphocytes displaying perinuclear space (arrowhead), and retracted cytoplasm (curved arrow). (C) Non-plastinated specimen showing red blood cells (RBCs) and lymphocytes nucleus (N) are firmly bound. (D) Plastinated sample showing widening of intercellular spaces (asterisks). (E) Non-plastinated macrophage with kidney-shaped nucleus (N) and rough endoplasmic reticulum (RER). (F) plastinated macrophage exhibiting dilated RER (diamond arrow).

Testis

Light microscopic results

The non-plastinated testis of the camel was enclosed by a fibrous capsule known as the tunica albuginea, which was dense and thick. Beneath this capsule, there was a layer called the tunica vasculosa, which was highly vascular and contained blood vessels supplying the testes (Fig. 5A). The testicular parenchyma consisted of interstitial tissue, which contained Leydig cells and was rich in blood vessels, and dense connective tissue within the seminiferous tubules was organized (Fig. 5C). The seminiferous tubules had a wide lumen and were covered with germinal epithelium, containing various stages of spermatogenic cells. They were supported by a straight and tightly attached basement membrane (Fig. 5E). The basement membrane was supported by contractile myoid cells (Fig. 5G). In contrast, the plastinated testicular capsule became thinner (Fig. 5B). The testicular parenchyma showed shrinkage, creating peri-tubular spaces around seminiferous tubules (Fig.5 D). The basement membrane of the plastinated tubules became irregular and undulating, while the lumen of tubules exhibited narrowing (Fig. 5F). Also, in high magnification, the basement membrane revealed separation from the germinal cell layers and leaving gaps (Fig. 5H).

Transmission electron microscopic results

An ultrastructural analysis of the non-plastinated seminiferous tubule in the camel's testis revealed a thin, straight tubular basement membrane

lined with flat myoid cells. Sertoli cells, which rested on the basement membrane, had oval nucleus and contained various cytoplasmic organelles such as mitochondria and lysosomal bodies, with clearly defined cytoplasmic membranes separating different germinal cells (Fig. 6A). These germinal cells, including spermatogonia, that showed circular nucleus and clear nuclear membrane with visible organelles (Fig. 6C). Additionally, the sperm and spermatid cell with its acrosomal cap (Fig. 6E). All testicular cells maintain their structural integrity and cellular architecture (Fig. 6G). On the other hand, the plastinated Sertoli cell rested on an irregular basement membrane with enlarged myoid cell and no visible organelles or cell membrane (Fig. 6B). The cytoplasm of Spermatogonium became shrunken, leaving it surrounded by a perinuclear space and appeared of cytoplasmic vacuole (Fig. 6D). Also, the spermatid cell revealed extra cytoplasmic vacuole (Fig. 6F). Additionally, Sertoli cell nucleus appeared with folded envelope and widening of intercellular space (Fig. 6H). The intercellular matrix underwent shrinkage, which resulted in the formation of a perinuclear space around cells (Fig. 6I). At high magnification of Sertoli cell, its nuclear envelope became irregular. The basal lamina exhibited a thick, wavy, and irregular appearance, with slightly contracted, enlarged myoid cells and a gap between the cellular lamina layers (Fig. 6J).

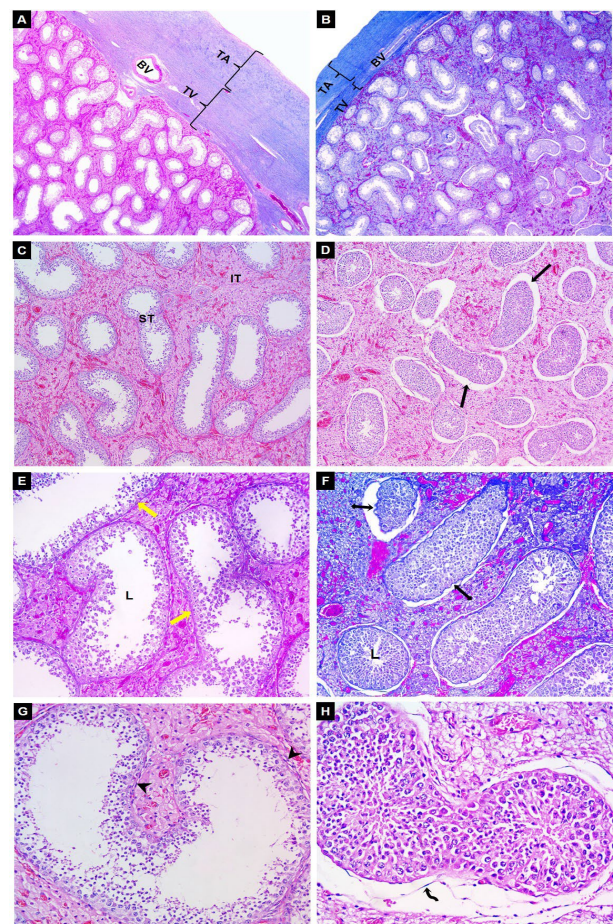


Fig. 5. Photomicrographs of plastinated and non-plastinated testes. (A) Non-plastinated testis showing dense capsule of tunica albuginea (TA) and tunica vasculosa (TV) with blood vessels (BV). (B) Plastinated testis show thinner capsular layers. (C) Non-plastinated parenchyma showing interstitial tissue (IT) surrounding seminiferous tubules (ST). (D) Plastinated tubules had peri-tubular space (black arrow). (E) Non-plastinated tubules showing wide lumen (L) and stratified germinal epithelium rested on a straight basement membrane (yellow arrow). (F) Plastinated tubules showing an irregular basement membrane (diamond arrow) and narrow lumen. (G) High magnification of non-plastinated tubules revealed intact basal membrane lined with myoid cells (arrowhead). (H) High magnification of plastinated tubules exhibited separation of the basement membrane (curved arrow). (A, B) at X40 magnification with MTC, (C, D) at X100 magnification with H&E, (E, F) at X200 magnification with MTC, (G, H) at X400 magnification with H&E staining.

Discussion

The current study investigated the effect of different chemicals in each step of the Elnady plastination technique on the spleen and testis

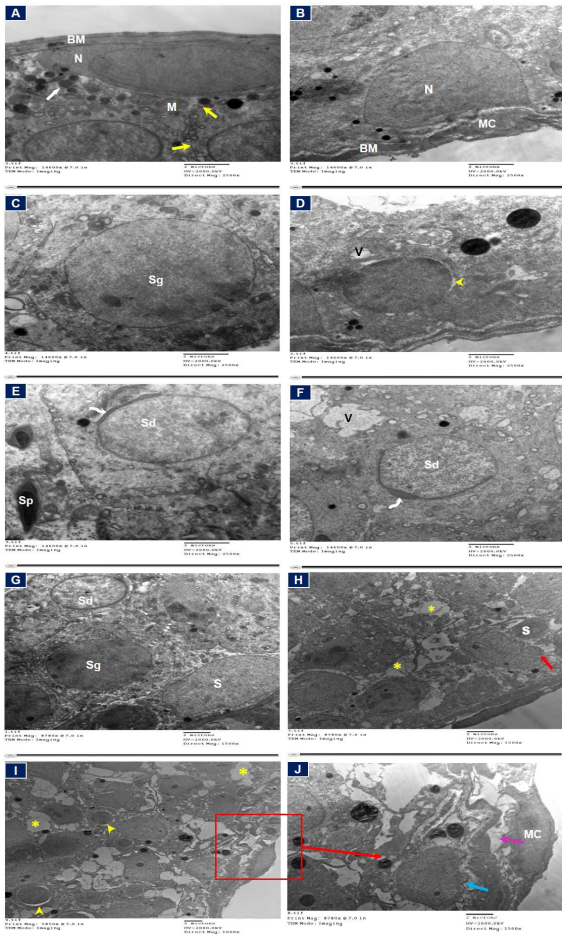


Fig. 6. Transmission electron micrographs of plastinated and non-plastinated testes. (A) Non-plastinated seminiferous tubule with a Sertoli cell nucleus (N) resting on a straight basement membrane (BM) with visible organelles as mitochondria (M), lysosomes (thick white arrow), and clear cell membrane (yellow arrow). (B) Plastinated Sertoli cell on an irregular basal lamina, with an enlarged myoid cell (MC). (C) Non-plastinated spermatogonia (Sg) with a distinct nuclear membrane and visible organelles. (D) Plastinated spermatogonium with a perinuclear space (yellow arrowhead) and cytoplasmic vacuole (V). (E) Non-plastinated spermatid nucleus (Sd), acrosomal cap (curved arrow), and clear cell membrane separating it from sperm (Sp). (F) Plastinated spermatid with ill-defined cytoplasmic membrane and vacuolation (V). (G) Non-plastinated seminiferous tubule showing normal arrangement of Sertoli cells (S) and other germ cells with clear structure. (H) Plastinated specimen of Sertoli cell nucleus with a folded envelope (red arrow) and increased intercellular space (asterisks). (I) Plastinated seminiferous tubule revealed large intercellular spaces (asterisks) and perinuclear spaces (yellow arrowhead). (J) High magnification of plastinated Sertoli cell showing irregular nuclear membrane (blue arrow), gap between layers (pink arrow), and enlarged myoid cell (MC).

of the camel. The formalin fixation phase showed a noticeable increase in the weight of the testis. At the same time, the spleen exhibited reduction as its hemopoietic character led to the oozing of the blood after formalin injection.

The acetone dehydration step is a crucial part of the plastination process, as it results in the shrinkage of the preserved organs (Hollada, 1988; Sajjarengpong *et al.*, 2011). So, in this work, there was noticeable and substantial tissue shrinkage in the acetone step; this came in agreement with García-Garza *et al.* (2021). In addition, the defatting and dehydration effects of the acetone caused the acetone bath to become contaminated with fats, resulting in a yellowish color to the bath. These findings were consistent with Grondin *et al.* (1997).

Furthermore, the glycerin impregnation phase also showed shrinkage, as the hydrophobic nature of glycerin prevents water from entering the cells. These results were aligned with Xia *et al.* (2022). By the end of the plastination treatment, we observed that the testis experienced more pronounced shrinkage compared to the spleen, possibly due to the fibrinous characteristics of the testicular parenchyma and capsule, which displayed contracted fibers, leading to the shrinkage. These outcomes were matched with Elnady (2016).

The gross anatomical identification in our investigation revealed that the spleen of the camel was C-shaped with a reddish-brown coloration

similar to that mentioned by Maher and Noor (2018). The mean camel spleen weight was 475.83 ± 38.00 g, which is approximately near to the weight reported by Maina *et al.* (2014). On the other hand, the plastinated spleen showed differentiation in color, especially in the impregnation phase, which caused tissue darkness. This could be attributed to the glycerin action as recorded by Pichardo-Moliner *et al.* (2024).

Additionally, the camel testis in this work was white in color and covered by the thick connective tissue capsule of tunica albuginea, as documented by Mahendra *et al.* (2022). The average weight was 155.83 ± 24.98 g, which was in line with Smuts and Bezuidenhout (1987). In contrast, the plastinated testis exhibited greater transparency in its capsule, which made the blood vessels of the tunica vaginalis more visible. These observations may be due to the plasticizing and transparent properties of glycerin (Nashed *et al.*, 2003; El-Shafey *et al.*, 2022).

Moreover, the histological analysis in the present study helped distinguish between plastinated and non-plastinated tissues. Under the light microscope, the non-plastinated camel spleen showed a thick connective tissue capsule surrounding the splenic parenchyma, composed of white and red pulp. These results were in line with Zidan *et al.* (2000a); Maina *et al.* (2014) and Maher and Noor (2018). Also, the collagen network present in the red pulp acts as a framework, helping to preserve the spleen's microarchitecture and providing significant tensile strength, as cited by Faller (1985). While, the plastinated spleen in this study showed some differences, particularly in the intensity of collagen fibers within the splenic capsule and parenchyma. This result was more detailed than that reported by Grondin *et al.* (1994) which referred to the shrinkage observed in the silicon plastination samples. This could be due to the shrinkage effects of glycerin, which leads to a decrease in the number of collagen fibers, similar to the reduction of corneal collagen fibrils in glycerin preserved sample as noted by Xia *et al.* (2022).

Through our study, the non-plastinated testis displayed a thick testicular capsule and seminiferous tubules arranged in a typical manner, containing spermatogenic cells and surrounded by a straight, tightly attached basement membrane. These results were supported by Singh and Bharadwaj (1978) and Mahmud *et al.* (2015). Conversely, the plastinated testis, which has not been extensively studied in previous research, displayed contraction and irregularity in the collagen fibers of the basement membrane surrounding the seminiferous tubules when stained with MTC stain.

According to Ahmed *et al.* (2024), the plastinated specimens from Elnady do not interfere with TEM examination. Therefore, in our study, TEM was used to confirm the histological changes observed under the light microscope. The non-plastinated camel spleen showed ultrastructural details of various cells, including lymphocytes and macrophages, which displayed distinct and well-defined cytoplasmic organelles and a uniform cytoplasmic matrix. These findings were in agreement with the TEM results of the camel spleen as mentioned by Zidan *et al.* (2000b) and the buffalo spleen as cited by Rashad *et al.* (2020). On the other hand, the plastinated spleen demonstrated strong potential for ultrastructural studies, aligning with previous research on silicon-plastinated spleen (Grondin *et al.*, 1994). Additionally, our outcomes revealed a decrease in the cytoplasmic volume and a change in the shape of the rough endoplasmic reticulum (RER) in macrophage cells. This might be attributed to the shrinkage caused by the chemical treatment involved in the plastination process.

In line with this, the TEM results of the non-plastinated camel testis revealed a straight basement membrane that plays a supportive role and regulates the exchange of nutrients between the testis and blood (Moniem *et al.*, 1980). Also, the Sertoli cells were situated on the membrane, with other spermatogenic cells positioned thereafter. These observations were consistent with Abd-elaziz *et al.* (2012). Unlike the plastinated testis that underwent to shrinkage, resulting in a disrupted basal membrane, unclear cell architecture, and a reduction in the amount of cytoplasmic connective tissue, which led to the formation of interstitial tissue spaces.

These findings in plastinated testes have not been reported in previous research.

Conclusion

The macroscopic changes of the Elnady plastination technique reflected the color changes during different phases. Also, the microscopic alternations, especially on the levels of connective tissue fibers of the spleen and the testis due to the shrinkage effect of acetone and glycerin. By considering the cost-effectiveness of used chemicals in this technique, as well as the shrinkage drawbacks, this study contributes to its wide application to minimize the harmful effect of formalin and decrease the numbers of executed animals for student education purposes.

Acknowledgments

The authors would like to thank all staff members of the Anatomy and Embryology Department, Faculty of Veterinary Medicine, Benha University, Egypt.

Conflict of interest

The authors have no conflict of interest to declare.

References

- Abd-elaziz, M.I., Kassem, A.M., Zaghloul, D.M., Derbalah, A.E., Bolefa, M.H., 2012. Ultrastructure of the interstitial tissue in the testis of the Egyptian dromedary camel (*Camelus dromedarius*). *Pakistan Veterinary Journal* 32, 65–69.
- Abdel-Maksoud, G., El-Amin, A.R., 2011. A review on the materials used during the mummification processes in ancient Egypt. *Mediterranean Archaeology and Archaeometry* 11, 129–150.
- Ahmed, O., Gaballa, M.M.S., Abumandour, M.M.A., Al-Otaibi, A.M., Choudhary, P., El-Shafey, A.A., 2024. Morphometric and histopathological evaluation of modified Elnady's plastinated tissue compared to non-plastinated tissue: Highlighting its relevance for teaching and research. *Anatomia Histologia Embryologia* 53. <https://doi.org/10.1111/ahel.13046>
- Balta, J.Y., Cronin, M., Cryan, J.F., O'mahony, S.M., 2015. Human preservation techniques in anatomy: A 21st century medical education perspective. *Clinical Anatomy* 28, 725–734. <https://doi.org/10.1002/ca.22585>.
- Bancroft, J.D., Gamble, M., 2008. Theory and practice of histological techniques. Elsevier Health Sciences.
- Baygeldi, S.B., Şeker, U., Güzél, B.C., 2022. Histological Structure of the Plastinated Kidney Following Deplastination. *Harran Üniversitesi Veteriner Fakültesi Dergisi*. 11, 14–20. <https://doi.org/10.31196/huvfd.1023540>.
- Bernal, V., Aburto, P., Pérez, B., Gómez, M., Gutierrez, J.C., 2022. A Technical Note of Improvement of the Elnady Technique for Tissue Preservation in Veterinary Anatomy. *Animals* 12, 1111. <https://doi.org/10.3390/ani12091111>
- Dent, B.B., Forbes, S.L., Stuart, B.H., 2004. Review of human decomposition processes in soil. *Environmental Geology*. 45, 576–585. <https://doi.org/10.1007/s00254-003-0913-z>.
- El-Shafey, A., Magdy, Y., Hamad, A., Ahmed, O., 2022. Modified form of the Elnady Technique for tissues preservation. *Benha Veterinary Medical Journal* 41, 56–60. <https://doi.org/10.21608/bvmj.2021.95641.1470>.
- Elnady, F., 2016. The Elnady Technique: An innovative, new method for tissue preservation. *ALTEX* 33, 237–242. <https://doi.org/10.14573/altex.1511091>.
- Elshaer, N.S.M., Mahmoud, M.A.E., 2017. Toxic effects of formalin-treated cadaver on medical students, staff members, and workers in the Alexandria Faculty of Medicine. *Alexandria Journal of Medicine* 53, 337–343. <https://doi.org/10.1016/j.ajme.2016.11.006>.
- Faller, A., 1985. Splenic architecture reflected in the connective tissue structure of the human spleen. *Experientia* 41, 164–167. <https://doi.org/10.1007/BF02002609>.
- García-Garza, R., Salas-Treviño, D., Soto-Patiño, F.A., González-Murillo, E.A., Castelan-Maldonado, E.E., Saucedo-Cárdenas, O., Romero-Díaz, V.J., Velázquez-Gauna, S.E., Soto-Domínguez, A., 2021. Fast acetone tissue processing of human organs provides tissue characteristics equal to conventional processing. *Biotechnic and Histochemistry* 96, 20–27. <https://doi.org/10.1080/10520295.2020.1752935>.
- Grondin, G., Grondin, G.G., Talbot, B.G., 1994. A study of criteria permitting the use of plastinated specimens for light and electron microscopy. *Biotechnic and Histochemistry* 69, 219–234. <https://doi.org/10.3109/10520299409106291>.
- Grondin, G., Henry, R.W., Janick, L., Bérubé, S., 1997. Reclamation of acetone in plastination laboratories: A simple and inexpensive method. *Cells Tissues Organs* 158, 26–29. <https://doi.org/10.1159/000147905>.
- Holladay, S.D., 1988. Experiments in Dehydration Technique. *Journal of the International Society for Plastination* 2, 17–20. <https://doi.org/10.56507/rsdz6598>.
- Islam, R., Ayman, U., Sultana, N., 2021. Histological Architectures and Biometric Characteristics of Indigenously Plastinated Organs of Goat. *International Journal of Morphology* 39, 795–765.
- Mahendra, K.S., Sanjeev Joshi, Pankaj Kumar Thanvi, Aruna Panwar, Devendra Singh, S. and R.K.S., Abstract, 2022. Gross anatomical study on the testes of camel (*Camelus dromedarius*). *The Pharma Innovation Journal* 11, 2673–2679 ISSN.
- Maher, M., Noor, A., 2018. Gross anatomical, radiographic and ultra-structural identification of splenic vasculature in some ruminants (camel, buffalo calf, sheep and goat). *International Journal of Advanced Research in Biological Sciences* 5, 44–65. <https://doi.org/http://dx.doi.org/10.22192/ijarbs.2018.05.02.006>
- Mahmud, Onu, J.E., Shehu, S.A., Umaru, M.A., Danmaigoro, And, A., Bello, A., 2015. Comparative gross and histological studied on testis of one-humped camel bull, uda ram and red sokoto buck. *International Journal of Multidisciplinary Research and Information* 1, 81–84.
- Maina, M., Usende, I., Igwenagu, E., Onyiche, T., Yusuf, Z., Ntung, N., 2014. Gross, Histological and Histomorphometric Studies on the Spleen of One Humped Camel (*Camelus dromedarius*) Found in the Semi-arid Region of North Eastern Nigeria. *Journal of Veterinary Advances*. 4, 703–711. <https://doi.org/10.5455/jva.20141025045543>.
- Moniem, K.A., Tingari, M.D., Kuenzel, E., 1980. The fine structure of the boundary tissue of the seminiferous tubule of the camel (*Camelus dromedarius*). *Acta Anatomica (Basel)*. 107, 169–176. <https://doi.org/10.1159/000145239>.
- Nashed, G., Rutgers, R.P.G., Sopade, P.A., 2003. The plasticisation effect of glycerol and water on the gelatinisation of wheat starch. *Starch/Stärke* 55, 131–137. <https://doi.org/10.1002/star.200390027>
- Ostrom, K., 1987. Fixation of Tissue for Plastination: General Principles. *Journal of the International Society for Plastination* 1, 3–11. <https://doi.org/10.56507/WLZH2223>
- Pichardo-Moliner, M.R., Jardon-Xicotencatl, S., Oliver-González, M.R., García-Tovar, C.G., 2024. Implementation of a New Solution for the Preservation of Anatomical Specimens Made of Non-Toxic Substances. *Open Journal of Veterinary Medicine* 14, 56–67. <https://doi.org/10.4236/ojvm.2024.143005>.
- Rashad, E., Hussein, S., Bashir, D.W., Ahmed, Z.S.O., Maher, M.A., El-Habbak, H., 2020. Anatomical, histological, histochemical, scanning and transmission electron microscopic studies on water buffalo (*Bubalus bubalis*) spleen. *Journal of Critical Reviews* 7, 1751–1774. <https://doi.org/10.31838/jcr.07.17.223>.
- Reina-De La Torre, F., Rodríguez-Baeza, A., Doménech-Mateu, J.M., 2004. Setting up a plastination laboratory at the Faculty of Medicine of the Autonomous University of Barcelona. *European Journal of Anatomy* 8, 1–6.
- Sajjarengpong, K., Chuesiri, P., Prachammuang, P., Phisiriuenyong, P., 2011. Efficacy of Acetone and Ethanol in Dehydrating Canine Body Sheets :Before and After Resin Coating. *Thai The Thai Journal of Veterinary Medicine* 41, 487–492. <https://doi.org/10.56808/2985-1130.2341>.
- Singh, U.B., Bharadwaj, M.B., 1978. Histological and histochemical studies on the testis of camel (*Camelus dromedarius*) during the various seasons and ages: Part II. *Cells Tissues Organs* 101, 280–288. <https://doi.org/10.1159/000144978>.
- Smuts, M.M.S., Bezuidenhout, A.J., 1987. Anatomy of the dromedary, Oxford science publications TA - TT -. Clarendon Press; Oxford University Press, Oxford [Oxfordshire], New York SE. <https://worldcat.org/title/12944874>.
- Sora, C., Traxler, H., 1999. P40 Plastination of Human Brain Slices: Comparison between Different Immersion and Impregnation Conditions. *Journal of the International Society for Plastination* 14, 22–24. <https://doi.org/10.56507/xlsj5724>.
- Tizro, P., Choi, C., Khanlou, N., 2019. Sample Preparation for Transmission Electron Microscopy pp. 417–424. https://doi.org/10.1007/978-1-4939-8935-5_33.
- Xia, F., Zhao, J., Fu, D., Qin, B., Chen, Z., Zhao, Y., Shen, Y., Hou, J., Zhou, X., 2022. Comparison of the effects of temperature and dehydration mode on glycerin-based approaches to smile-derived lenticule preservation. *Cornea* 41, 470–477. <https://doi.org/10.1097/ICO.0000000000002846>.
- Yunus, H.A., Ekim, O., Bakici, C., Batur, B., Çakir, A., 2022. From toxic cadavers to biosafe specimens: a brief history of plastination in veterinary anatomy. *Veteriner Hekimler Derneği Dergisi*. 93, 158–165. <https://doi.org/10.33188/vetheder.998978>.
- Zidan, M., Kassem, A., Pabst, R., 2000. Megakaryocytes and platelets in the spleen of the Dromedary camel (*Camelus dromedarius*). *Anatomia Histologia Embryologia* 29, 221–224. <https://doi.org/10.1046/j.1439-0264.2000.00268.x>.
- Zidan, M., Kassem, A., Dougbag, A., El Ghazzawi, E., El Aziz, M.A., Pabst, R., 2000. The spleen of the one humped camel (*Camelus dromedarius*) has a unique histological structure. *Journal of Anatomy* 196, 425–432. <https://doi.org/10.1046/j.1469-7580.2000.19630425.x>